Rescue of Lethal Subunits into Functional K^+ Channels

M. Taglialatela,* J. P. Payne,‡ J. A. Drewe,* and A. M. Brown*
Departments of *Molecular Physiology and Biophysics and ‡Medicine, Section of Cardiology, Baylor College of Medicine, Houston, TX 77030 USA

ABSTRACT In a chimeric, voltage-dependent K^+ channel (CHM), the valine at position 369 and the leucine at position 374 interact within the pore or P-region to regulate ion permeation and block. Here we show that the point mutation, CHM V369L, abolished channel function whereas previous experiments showed that CHM V369 and CHM V369I are functional. Coinjection of "lethal" CHM V369L cRNA with CHM L374V cRNA but not CHM cRNA generated functional heteromultimers. The whole-cell Rb^+/K^+ conductance ratio was 2.98 ± 0.43 for CHM L374V and was reduced to 0.87 ± 0.04 for the coexpressed CHM V369L and CHM L374V subunits. When single-channel currents were recorded, a single class of CHM V369L/CHM L374V heteromultimers was identified. This class was readily distinguishable from CHM L374V homomultimers by K^+ conductance, gating, and blockade by internal tetraethylammonium. Coinjection experiments at various RNA ratios suggest that the CHM V369L/CHM L374V heteromultimer, assuming it to be a tetramer, was composed of three CHM L374V subunits and one CHM V369L subunit. It appears that in the critical P-region of CHM position 369 may tolerate only one leucine.

INTRODUCTION

The notion that functional K^+ channels assemble as multimers, originally suggested by the sequence homology between K^+ channels (Schwartz et al., 1987) and each of the four domains of Na^+ (Noda et al., 1984) and Ca^{++} (Tanabe et al., 1987) channels, has now received extensive experimental support. *Xenopus* oocytes coinjected with cRNAs encoding for K^+ channels which had different gating (Isakoff et al., 1990; Ruppersberg et al., 1990) and/or pharmacological properties (Christie et al., 1990; Kavanaugh et al., 1992; MacKinnon, 1991) displayed macroscopic currents consistent with the expression of heterotetrameric channels with phenotypes intermediate between the two parent homomeric channels. Assembly of different subunits has been proposed as one of the possible mechanisms controlling K^+ channel heterogeneity in vivo (Salkoff et al., 1992; Po et al., 1993). One constraint on assembly is that subunits must belong to the same K^+ channel subfamily and the recognition mechanism is thought to reside in a conserved stretch in the NH_2 terminus (Li et al., 1992; Shen et al., 1993).

A major part of the ion conduction pathway or pore or P-region of voltage-gated K^+ channels has been localized to the linker between putative transmembrane segments S_5 and S_6 (Yellen et al., 1991; Yool and Schwartz, 1991; Hartmann et al. 1991). A chimeric channel (CHM) (Hartmann et al., 1991) in which a 21-amino acid segment from the delayed rectifier Kv 3.1 (Yokoyama et al., 1989) was substituted for the homologous region of the delayed rectifier Kv 2.1 (Frech et al., 1989) had the single-channel K^+ conductance and external and internal tetraethylammonium (TEA) blockade of the donor Kv 3.1 channel, distinct from that of the host Kv 2.1. Single point reversions in the CHM channel identified two mutations in the P-region, V369I and L374V, which affected permeation, gating, and TEA blockade (Kirsch et al., 1992a,b). A double mutant involving both of these residues (V369I + L374V) generated a phenotype clearly distinct from the two novel phenotypes produced by single mutations (V369I and L374V), indicating that these residues interact within the same subunit. In addition, experiments with the coinjection CHM V369I and CHM L374V cRNAs have suggested that these two pore residues can interact across subunit boundaries (Kirsch et al., 1992c).

Most substitutions at position 369 (DeBiasi et al., 1993) in both CHM and Kv 2.1 channels resulted in functional channel expression. One of the "lethal" mutations, CHM V369L, was particularly interesting, since at position 374 either V or L was readily accommodated. In addition, the loss of function was produced by a substitution that involved only a small decrease in hydrophilicity and a small increase in volume of 25 $Å^3$ (Richards, 1977).

Our previous work has shown the importance of L or V at 374 to ion conduction and gating and we wondered whether the simultaneous presence of two Ls at 369 and 374 of the same subunit caused CHM V369L to be lethal. The aim of the present study was therefore to investigate at the single-channel level the possibility that lethal CHM V369L subunits could be rescued into functional heterotetrameric channels when coexpressed with subunits such as CHM L374V. Our results showed that lethal CHM V369L subunits were incorporated into functional heteromeric channels with CHM L374V subunits. The rescue process displayed a high degree of specificity, since only one class of heteromeric channels could be identified. Furthermore, the original CHM with L at 374 did not appear to form functional heteromultimers with CHM V369L subunits.

Received for publication 27 May 1993 and in final form 10 September 1993.
Address reprint requests to Dr. M. Taglialatela, Dept. of Molecular Physiology and Biophysics, Baylor College of Medicine, One Baylor Plaza, Houston, TX 77030.
© 1994 by the Biophysical Society
0006-3495/0/01/179/12 $2.00

MATERIALS AND METHODS

Standard recombinant DNA techniques and site-directed mutagenesis.

Standard methods of plasmid DNA preparation, site-directed mutagenesis and DNA sequencing were used (Kirsch et al., 1992a; Maniatis et al., 1982), and the design of the CHM channel between Kv 2.1 and Kv 3.1 has been previously described (Hartmann et al., 1991). CHM and its mutants were propagated in the plasmid vector pBluescript SK(−) in *Escherichia coli* Xl1-blue (Stratagene, LaJolla, CA). Single-stranded DNA templates were subcloned into M13 mp19 single-stranded phagemid, and the mutagenesis reaction was carried out by means of a commercially available kit (Amersham, Amersham, England). The mutated region of the M13 construct was then subcloned back into the pBluescript construct. The region spanning the cloning sites was then sequenced to verify the presence of the mutation.

In vitro transcription of the mRNAs and oocyte injection.

Preparation of cRNAs utilizing the T7 RNA polymerase and in vitro capping of the RNAs has been previously described (Joho et al., 1990). The RNA concentration was quantified by [^{32}P]UTP incorporation. Stage V–VI *Xenopus* oocytes were injected with 46 nl of 0.002–200 ng/μl cRNA solutions in 0.1 M KCl and incubated at 19°C in modified Barth's solution. For whole-cell measurements, the follicular layer surrounding the eggs was manually removed at least 4 h before recording. For single-channel recording, the vitelline membrane was also manually removed. Coinjection of two cRNAs encoding for different subunits was performed by mixing various concentrations of the cRNAs obtained from separate transcription reactions. For the coinjection ratio experiments described in Fig. 7, similar results were obtained when oocytes were injected with two separate batches of cRNAs encoding for each monomer, each transcribed from two separate plasmid preparations. Unless otherwise stated (see Fig. 7 and section *ii* of the Appendix), for coinjection experiments with two RNA species, the RNA concentration ratio is expressed as a mass (w/w) ratio.

Electrophysiology

Whole-cell measurements

Two to 5 days after the injection, the follicular cell layer was manually removed and oocytes were voltage-clamped using a commercial two-electrode voltage clamp amplifier (Dagan 8500, Dagan Corp., Minneapolis, MN). Current and voltage electrodes were filled with 3 M KCl, 10 mM HEPES (pH 7.4; ≈1 MΩ resistance). The bath solutions were: low K^+-MES (120 mM *N*-methyl-D-glucamine, 120 mM MES, 2.5 mM KOH, 2 mM $Mg(OH)_2$, and 10 mM HEPES, pH 7.4); high K^+-MES (22.5 mM *N*-methyl-D-glucamine, 122.5 mM MES, 100 mM KOH, 2 mM $MgOH_2$, and 10 mM HEPES, pH 7.4); high Rb^+-MES (22.5 mM *N*-methyl-D-glucamine, 122.5 mM MES, 100 mM RbOH, 2 mM $MgOH_2$, and 10 mM HEPES, pH 7.4). The PClamp system (Axon Instruments, Foster City, CA) was used for the generation of the voltage pulse protocols and for data acquisition. Linear leakage and capacity currents were corrected on line using the P/4 subtraction method.

Single-channel currents

Single-channel currents were recorded from inside-out membrane patches using oocytes dissected free of the vitelline envelope and micropipettes of 2–5 MΩ resistance that were fire-polished and Sylgard-coated (Dow-Corning, Midland MI). The pipette solution was Mg-Ringer's: 120 mM NaCl, 2.5 mM KCl, 2 mM $MgCl_2$, and 10 mM HEPES, pH 7.2. Holding and test potentials applied to the membrane patch are reported as conventional absolute intracellular potentials assuming that the oocyte resting potential was zeroed by a bathing solution containing either 100 mM KCl (Iso-K^+) or 100 RbCl (Iso-Rb^+), and 10 mM EGTA, 10 mM HEPES, pH 7.2. Data were low-pass filtered at 1 kHz (−3 dB, four-pole Bessel filter) prior to digitization at 5 kHz. Channels were activated with rectangular test pulses from negative holding potentials (−80 mV to −120 mV). Current records were corrected for capacitative and leakage currents by subtracting the smoothed average of records lacking channel activity ("null traces").

Data were analyzed as follows. Single-channel currents were idealized using an algorithm which uses a *dI/dt* threshold for identifying transitions between closed and open states (VanDongen, 1992). Transition events were collected into amplitude distribution histograms, which were then fitted by Gaussian functions using a maximum likelihood estimate. In a second pass through the data, idealized openings were constructed using a threshold set at one-half the amplitude of the unitary current. Open and closed interval durations of the idealized data were collected into distribution histograms that were fit by monoexponential or, if necessary, pluriexponential decay functions using a maximum likelihood estimate. Events of <0.5 ms duration were excluded from the histogram to avoid truncation errors introduced by the limited frequency response of the system. Where appropriate, data are expressed as mean ± SE. Both whole-cell and single-channel experiments were performed at room temperature (22–24°C) in a recording chamber that was continuously superfused with bath solution at a rate of 2 ml/min.

RESULTS

Whole-cell currents from oocytes injected with the cRNAs for CHM L374V, CHM V369L, and a mixture of CHM V369L and CHM L374V

In Fig. 1 *A* are shown macroscopic current responses from voltage-clamped *Xenopus* oocytes injected with CHM L374V cRNA. Depolarization of the oocyte membrane from −80 mV to +40 mV resulted in the rapid activation of a K^+-selective outward current which inactivated by less than 5% during the 150–200 ms pulse. When the voltage of the cell was stepped in the hyperpolarizing direction, the channel deactivation time constant was clearly faster at more negative potentials, reaching a value of about 4–5 ms at −80 mV. This value is similar to the deactivation time constant recorded from macropatch measurements and single-channel ensemble records obtained under the same recording conditions (see later). Instantaneous current/voltage (I/V) relationships were derived by extrapolating tail currents at each potential to the beginning of the hyperpolarizing pulse and normalized to the value at +40 mV to facilitate comparison among cells with different levels of expressed currents. As shown in the left panel of Fig. 1 *D*, with high K^+ outside the instantaneous I/V was approximately linear between −80 mV and +40 mV (Kirsch et al., 1992b). When external K^+ ions were substituted with an equivalent concentration (100 mM) of Rb^+ ions, the outward currents, carried by K^+ ions, were unaffected; however, the inward currents, carried by Rb^+, were much larger than the inward K^+ currents. The instantaneous I/V showed marked inward rectification, as shown in the left panel of Fig. 1 *D*. The tail current relaxation was also slower when the currents were carried by Rb^+, an effect already observed for other K^+ channels (Sala and Matteson, 1991; Shapiro and DeCoursey, 1991). From a linear regression fit of the extrapolated inward tail current values between −50 mV and −80 mV, we estimated a limiting inward Rb^+/K^+ conductance ratio (g_{Rb^+}/g_{K^+}) of 2.98 ± 0.43 (n = 9), which

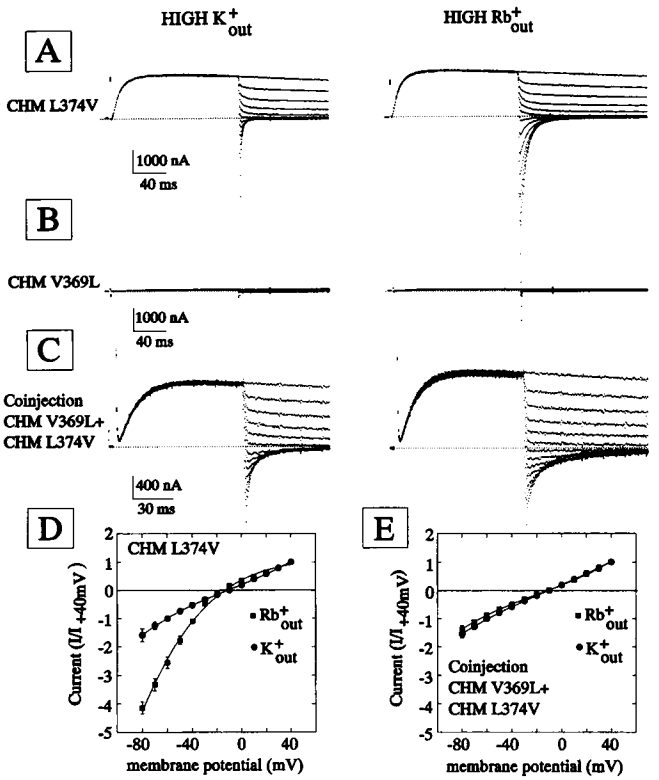

FIGURE 1 Whole-cell currents from oocytes injected with the cRNAs for CHM L374V, CHM V369L, and a mixture of CHM V369L and CHM L374V. (*A*) Whole-cell currents from *Xenopus* oocytes injected with CHM L374V, (*B*) CHM V369L, or (*C*) with a 1:1 (w/w) mixture of CHM L374V and CHM V369L cRNAs. Holding potential: −80 mV; test potential: +40 mV; return potential from +40 mV to −80 mV in −10 mV hyperpolarizing steps. External solution: high K^+-MES (*left panels*) or high Rb^+-MES (*right panels*). (*D* and *E*) Instantaneous I/V from oocytes injected with CHM L374V (*D*) or with a 1:1 mixture of CHM L374V and CHM V369L cRNAs (*E*). External (bath) solution: high K^+-MES (*filled circles*) or high Rb^+-MES (*filled squares*).

is identical to that obtained from outward single-channel currents between 0 mV and +40 mV (Table 1; Kirsch et al., 1992b).

By contrast, the injection of CHM V369L alone did not produce currents that could be distinguished from the endogenous currents. The voltage-dependent outward current was smaller than 150 nA at +40 mV (Fig. 1 *B*), even when cRNA concentrations 200 times higher than those used for CHM L374V were used. In addition, 49 patches were recorded from 4 batches of oocytes injected with maximal concentrations of CHM V369L cRNA, but no evidence for the expression of an heterologous channel was found.

However, if the cRNAs for CHM V369L and CHM L374V were coinjected together in a 1:1 mass concentration ratio, macroscopic currents were recorded and were different from currents generated by the injection of CHM L374V cRNA alone (Fig. 1 *C*). The currents remained K^+ selective, since the reversal potential changed with external K^+ concentration in accordance with the Nernst equation. However, the large increase in inward conductance observed in CHM L374V homomers upon changing the external solution from high K^+-MES to high Rb^+-MES, was not observed, and the ratio g_{Rb^+}/g_{K^+} was 0.87 ± 0.04 (n = 7, Fig. 1 *E*).

These whole-cell coinjection results suggested that functional heteromultimeric channels had formed between CHM V369L and CHM L374V, which had conduction properties different from those of CHM L374V homomers. Interestingly, whole-cell currents were not expressed after injection of cRNA encoding for the double mutant CHM V369L + L374V or after coinjection of CHM V369L with the double mutant CHM V369L + L374V (data not shown).

It should be underlined that the experiments described were performed with a CHM V369L mutation carrying a COOH terminus deletion of 318 amino acids (CHM V369L ΔC 318). The COOH terminus deletion did not appear to affect the results obtained as well as their interpretation for the following reasons:

1. Injection of cRNAs encoding for both full-length and ΔC 318 CHM V369L mutation did not generate functional channel expression.
2. When compared to the full-length version, the COOH terminus deletion did not cause any change in macroscopic and single-channel K^+ currents or gating of CHM V369I (DeBiasi et al., 1993).
3. Injection of about 1 nM of cRNA encoding for either the full-length or the ΔC 318 version of CHM L374V generated the same amount of macroscopic current. On day 3 after the injection, the peak outward current at +40 mV was 2.889 ± 193 μA (n = 5) for the full-length version and

TABLE 1 Biophysical and pharmacological properties of the CHM wild-type homomer, of the CHM L374V homomer, and of the CHM V369L/CHM L374V heteromultimer

	CHM WT* Homomer	CHM L374V Homomer	CHM V369L/CHM L374V Heteromultimer
g_K (pS)	21.9 ± 1.9 (16)	4.8 ± 0.2 (16)	14.8 ± 0.7 (16)
g_{Rb} (pS)	6.8 ± 1.4 (6)	15 ± 1.3 (5)	12.3 ± 1.1 (11)
g_{Rb}/g_K	0.17‡	2.98‡	0.87‡
Mean open time (ms)	40.7 ± 3.9 (8)	5.4 ± 0.3 (7)	13.3 ± 1.8 (5)
P_O (%)	80	7.8	68
K_d internal TEA (mM)	3.0 (K_{in})§	0.15 (Rb_{in})§	0.7 (K_{in})§
K_d external TEA (mM)	0.3	0.4	0.4

* Data for the CHM homomeric channel are from Kirsch et al. (1992a) and Kirsch et al. (1992b).

‡ These values are from macroscopic current measurements, as they appear in the text.

§ For a discussion of the effect of different permeant ions on internal TEA block, see Taglialatela, et al., (1993).

2.603 ± 193 μA (n = 7) for the ΔC 318 construct. The limiting inward Rb^+/K^+ conductance ratio (g_{Rb^+}/g_{K^+}, see below) of the full-length version and the ΔC 318 construct of CHM L374V mutation was identical, being 2.98 ± 0.43 (n = 9) and 3.07 ± 0.45 (n = 5), respectively.

4. Also the single-channel gating and permeation properties (see next paragraph) were indistinguishable between the full-length or the ΔC 318 version of CHM L374V. As previously described, oocytes coinjected with a 1:1 mass concentration ratio of cRNAs encoding for CHM V369L ΔC 318 and CHM L374V full length had a g_{Rb^+}/g_{K^+} of 0.87 ± 0.04 (n = 7, Fig. 1 *E*). A similar value of 1.06 ± 0.05 (n = 3) was observed upon coinjection of an identical 1:1 mass concentration ratio of cRNAs encoding for the full-length CHM V369L and CHM L374V full length.

5. In wild type DRK1, removal of the 318 COOH terminus amino acids caused few changes in gating (VanDongen et al., 1990) or for internal TEA block (Taglialatela et al., 1991).

6. In experiments performed on Shaker channels (Li et al., 1992), no role was found for the COOH terminus in the multimeric channel assembly.

Taken together, these results suggest that the ΔC 318 mutation in the CHM V369L channel is likely to have minimal effects on channel assembly and function. For this reason, unless otherwise indicated, the CHM V369L ΔC 318 mutation is referred to as CHM V369L throughout the manuscript.

Single-channel currents from oocytes injected with the cRNA for CHM L374V or with mixtures of CHM V369L and CHM L374V

Fig. 2 *A* shows single-channel records obtained from an oocyte injected with CHM L374V cRNA. The homomeric CHM L374V single-channel features are very distinctive: the channels have small K^+ conductance, short open times (5.4 ± 0.3 ms, n = 7), and long closed times (32.4 ± 8 ms, n = 7), which are responsible for an average probability of opening (P_o) of only 7.8 ± 1% (n = 7).

In oocytes coinjected with the two cRNA species, in addition to the CHM L374V homomer already described, another channel species was present, as shown in Fig. 2 *B*. This channel had larger K^+ conductance, longer open times (13.3 ± 1.8 ms, n = 5), shorter closed times (5.1 ± 1.6 ms, n = 5), and larger overall P_o (66.7 ± 6.3%, n = 7). In Fig. 2 *C* are shown six traces from a different patch that contained at least two CHM L374V homomers together with another channel that has identical conductance and gating properties of the heteromer shown in isolation in Fig. 2 *B*. Identical heteromultimeric channels were obtained upon coinjection of CHM L374V cRNA with the ΔC 318 or the full-length version of the CHM V369L mutation (data not shown).

Fig. 3 shows a summary of all the single-channel patches analyzed from oocytes coinjected with CHM V369L and CHM L374V cRNAs. When the amplitude of the single-channel currents at 0 mV (Fig. 3 *A*) and +40 mV (Fig. 3 *B*) was plotted as a function of the number of observation performed, the distribution clearly showed two peaks, both at 0 and +40 mV. The peaks at 0.18 pA at 0 mV and at 0.35 pA at +40 mV corresponded to the homomeric CHM L374V channels since they are identical to those found in oocytes injected only with CHM L374V cRNA. On the other hand, we ascribe the larger peaks of 0.82 pA at 0 mV and 1.37 pA at +40 mV to the formation of a single class of heteromeric channel composed of both CHM V369L and CHM L374V subunits. From these data, it is evident that a single class of functional heteromultimeric channels are present with a single-channel outward conductance for K^+ between 0 and +40 mV of 14.8 ± 0.7 pS (n = 16), 3 times larger than the K^+ conductance of CHM L374V under identical conditions (4.8 ± 0.2 pS, n = 16) (Fig. 3 *C*).

If the same patches that had been previously exposed to internal K^+ ions, in order to allow the identification of the channel (CHM L374V homomer or CHM V369L/CHM L374V heteromer), were exposed to internal Rb^+ as the charge carrier, the differences in single-channel conductance between the two class of channels were dramatically decreased (Fig. 4). In fact, while in inside-out patches with Rb^+ on the internal side of the channel, the current carried by

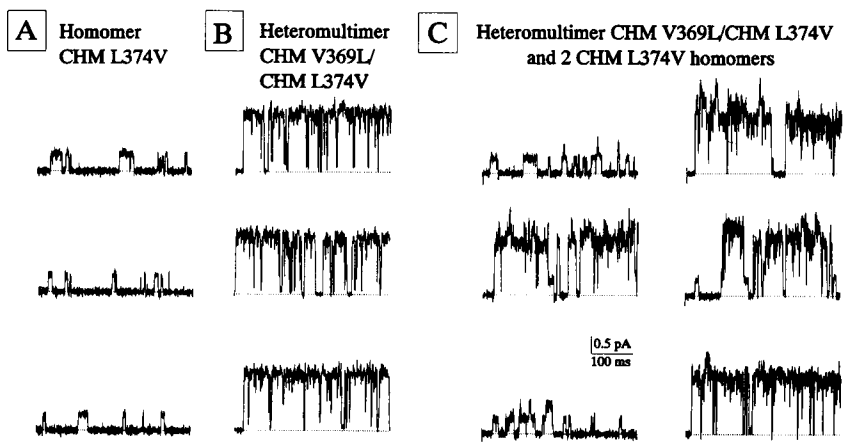

FIGURE 2 Single-channel currents from oocytes injected with the cRNA for CHM L374V or with CHM V369L and CHM L374V mixtures. (*A*) inside-out patch obtained from an oocyte injected with CHM L374V cRNA. (*B* and *C*) inside-out patches obtained from two oocytes injected with a 1:1 (w/w) mixture of CHM L374V and CHM V369L cRNAs. Test potential: +40 mV. External (pipette) solution: Mg-Ringer's; internal (bath) solution: Iso-K^+. Sampling: 5 kHz; filter: 1 kHz.

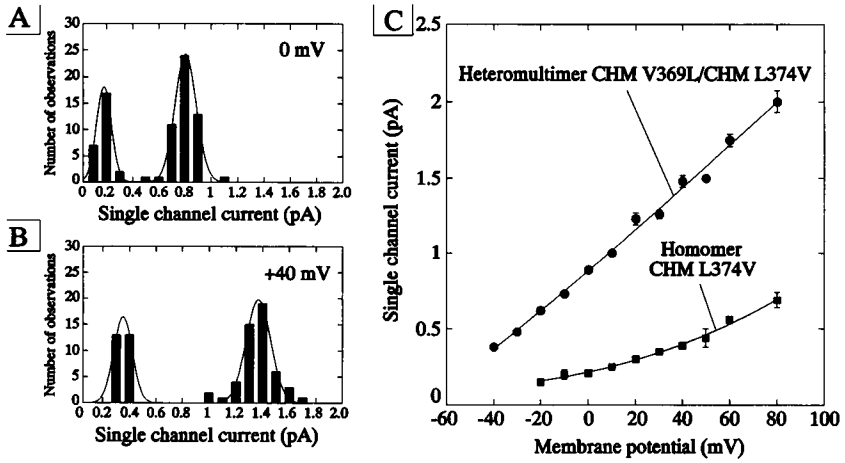

FIGURE 3 Distribution of the single-channel currents at 0 and +40 mV and single-channel I/V values from inside-out patches from oocytes injected with CHM V369L and CHM L374V cRNAs mixtures. The single-channel currents from oocytes injected with a 1:1 (w/w) concentration ratio of CHM L374V and CHM V369L cRNAs at 0 mV (*A*) and +40 mV (*B*) were binned (binwidth: 0.1 pA) and the numbers of counts per bin were plotted versus the single-channel amplitudes. The solid lines in both panels are the fits of the experimental data to a bimodal distribution, with mean values of 0.18 and 0.82 pA (*A*) and 0.35 and 1.37 pA (*B*). (*C*) single-channel I/V values for the CHM L374V homomer (*filled squares*) and for the CHM V369L/CHM L374V heteromer (*filled circles*). External (pipette) solution: Mg-Ringer's; internal (bath) solution: Iso-K^+.

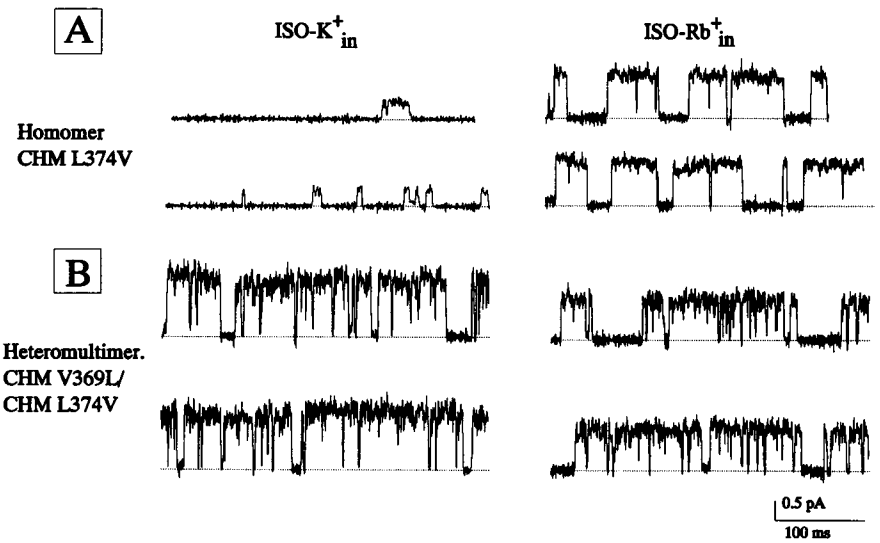

FIGURE 4 K^+ versus Rb^+ permeation in the CHM L374V homomer and in the CHM V369L/ CHM L374V heteromer. (*A*) inside-out patch obtained from an oocyte injected with CHM L374V cRNA. (*B*) inside-out patches obtained from oocytes injected with a 1:1 mixture of CHM L374V and CHM V369L cRNAs. Test potential: +40 mV. External (pipette) solution: Mg-Ringer's; internal (bath) solution: Iso-K^+ (*left panels*) or Iso-Rb^+ (*right panels*). Sampling: 5 kHz; filter: 0.5 kHz (Iso-K^+ traces of *A*) *or 1 kHz (Iso-*Rb^+ traces of *A*; Iso-K^+ and Iso-Rb^+ traces of *B*).

CHM L374V homomeric channels was increased with respect to K^+ (g_{Rb^+} was 15 ± 1.3 pS, n = 5); in the CHM V369L/CHM L374V heteromultimer, Rb^+ was only slightly less conducting than K^+ (g_{Rb^+} was 12.3 ± 1.1 pS, n = 11). Therefore, the single-channel ratio of the g_{Rb^+}/g_{K^+} was ≈3 for the CHM L374V homomultimer, whereas it was ≈0.8 for the CHM V369L/CHM L374V heteromultimer. A similar value (0.9) was also observed in whole-cell experiments in oocytes injected with a 1:1 mixture of the two cRNA species (see Fig. 1). This suggests therefore that in oocytes coinjected with a 1:1 ratio of CHM L374V to CHM V369L cRNA, most of the macroscopic current is carried by heteromeric channels formed by CHM V369L and CHM L374V; this is mainly due to the larger g_{K^+} and P_o of the heteromultimeric channel when compared to the CHM L374V homomultimeric channel.

In addition to the conductance changes, the data of Fig. 4 show that the substitution of K^+ for Rb^+ also caused dramatic changes in the gating of the channels. Particularly for CHM L374V homomers, the mean open time was considerably longer (about 15 ms) and the overall P_o increased.

Block by internal and external TEA in the CHM V369L and CHM L374V heteromultimer versus the CHM L374V homomultimer

The quaternary ammonium ion derivative TEA is known to block voltage-dependent K^+ channels by binding to two separate sites, which are accessible from the inside or the outside of the membrane (Armstrong, 1971; Taglialatela et al., 1991). In Fig. 5 are shown single-channel currents from inside-out patches containing either the CHM L374V homomultimer (*A*) or the heteromultimeric channel formed upon coinjection of CHM V369L and CHM L374V cRNAs (*B*). In the CHM L374V homomultimers, the exposure to

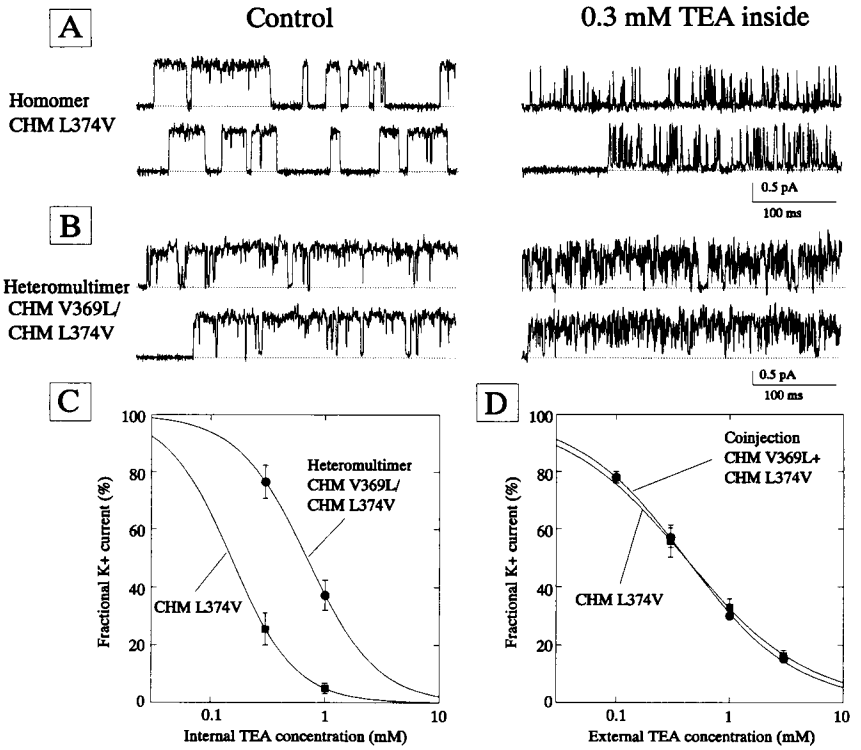

FIGURE 5 Internal and external TEA block in the CHM V369L and CHM L374V heteromultimer and the CHM L374V homomultimer. (*A*) Single-channel currents from inside-out patches containing either the CHM L374V homomultimer or (*B*) the heteromultimeric channel formed upon coinjection of CHM V369L and CHM L374V cRNAs exposed to the control condition (*left panels*) or to 0.3 mM internal TEA (*right panels*). Test potential: +40 mV. External (pipette) solution: Mg-Ringer's; internal (bath) solution: Iso-K^+ (*B*) or Iso-Rb^+ (*A*). Sampling: 5 kHz; filter: 1 kHz. (C) Dose-response relationship for internal TEA block at +40 mV in the CHM L374V homomer (*filled squares*) or the CHM V369L/CHM L374V heteromer (*filled circles*). Solutions as in *A* and *B*. (*D*) Dose-response relationship for external TEA block at +40 mV for the current of oocytes injected with the CHM L374V cRNA (*filled squares*) or with a 1:1 mixture of the cRNAs for CHM L374V and CHM V369L (*filled circles*). External (bath) solution: low K^+-MES.

internal TEA produced a concentration-dependent decrease in the mean open times with full interruptions of the single-channel currents and no effect on the channel first latencies, consistent with an open channel block mechanism (Armstrong, 1971; Taglialatela et al., 1991; Kirsch et al., 1991). On the other hand, the heteromultimer formed by CHM V369L and CHM L374V subunits was less sensitive to the block by internal TEA, mainly due to an increase in the OFF rate for the blocker (Taglialatela et al., 1993). The concentration dependence of the inhibition of the overall P_o by internal TEA is shown in *C*. The K_d values for internal TEA were 0.15 ± 0.06 mM (n = 3) for the CHM L374V homomer and 0.66 ± 0.08 mM (n = 5) for the CHM V369L/CHM 374V heteromultimer.

It should be noted that for CHM L374V homomers, the measurements were performed with Rb^+ as charge carrier, while for the heteromultimer formed by CHM V369L and CHM L374V, the conducting ion was K^+. This was necessary due to the very small g_{K^+} and short open times of the CHM L374V homomers. Furthermore, the fact that under these experimental conditions the two channels had identical conductances for the permeant ion (Rb^+ or K^+) makes it less likely that the observed differences in affinity for TEA resulted from possible differences in competition for the TEA blocking site between permeant ions and TEA. In fact, we have recently shown the existence of an inverse relationship between the g_{Rb^+}/g_{K^+} ratio and the ratio of the K_d values for internal TEA calculated with Rb^+ or K^+ ions as charge carriers (Taglialatela et al., 1993). Competition between permeant ions and internal TEA could explain the higher K_d reported for blockade by internal TEA in homomeric CHM L374V (Kirsch et al., 1992a), since the whole-cell experiments were performed with K^+ as charge carrier. Differences in channel gating between Rb^+ and K^+ could also be a factor.

While blockade by internal TEA differed between the homomeric CHM L374V channel and the heteromultimer composed of CHM V369L and CHM L374V subunits, external blockade by TEA did not seem to differ (Fig. 5 *D*). Dose responses for the blockade of outward K^+ currents by external TEA performed in oocytes injected either with CHM L374V alone or in combination with a 1:1 ratio of CHM V369L cRNA resulted in identical K_d values (0.377 ± 0.02, n = 5, and 0.405 ± 0.01, n = 3, respectively).

Whole-cell currents from oocytes injected with the cRNAs for CHM and a mixture of CHM V369L and CHM cRNAs

The results presented suggest that lethal subunits can be incorporated into functional heteromultimeric channels when coinjected together with functional subunits. In the following series of experiments we addressed the question of the specificity of this heteromultimeric assembly. Therefore, we coinjected *Xenopus* oocytes with equal amounts (w/w) of CHM V369L and CHM cRNA. At variance with homomultimeric CHM L374V channels, which conducted Rb^+ better than K^+ (see Fig. 1), homomultimeric CHM channels conduct K^+ better than Rb^+ (Fig. 6 *A*). From instantaneous I/V relationships, calculated as previously described, we estimated a g_{Rb^+}/g_{K^+} of 0.17 ± 0.02 (n = 4) (Fig. 6 *C*).

When coinjection experiments were performed with CHM and CHM V369L in a 1:1 w/w cRNA ratio, we

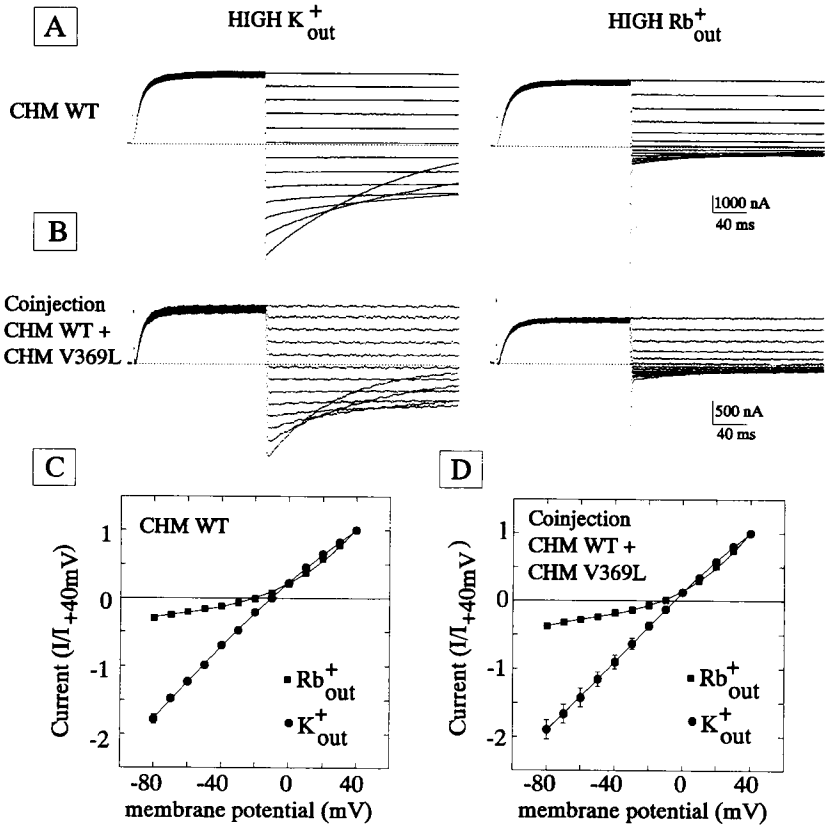

FIGURE 6 Whole-cell currents from oocytes injected with the cRNAs for CHM wild type or with a mixture of CHM V369L and CHM wild type. (*A*) Whole-cell currents from *Xenopus* oocytes injected with CHM wild type or (*B*) with a 1:1 (w/w) mixture of CHM wild type and CHM V369L cRNAs. Holding potential: −80 mV; test potential: +40 mV; return potential from +40 to −80 mV in −10 mV hyperpolarizing steps. External solution: high K^+-MES (*left panels*) or high Rb^+-MES (*right panels*). (*C* and *D*) Instantaneous I/V values from oocytes injected with CHM wild type (*C*) or with a 1:1 mixture of CHM wild type and CHM V369L cRNAs (*D*). External (bath) solution: high K^+-MES (*filled circles*) or high Rb^+-MES (*filled squares*).

failed to demonstrate any change in the g_{Rb^+}/g_{K^+} ratio (0.19 ± 0.02, n = 5) compared to the injection of CHM cRNA alone (Fig. 6 *B*).

Also, the affinity for external TEA block (K_d = 0.3 mM) was unchanged between oocytes coinjected with a 1:1 ratio of CHM and CHM V369L cRNAs and oocytes injected with CHM cRNA alone (Table 1). Taken together, these results with whole-cell experiments suggest that functional heteromultimers between CHM and CHM V369L do not form and that V369L subunits can only be rescued by L374V subunits. However, because of the large single-channel K^+ conductance and P_o of the homomeric CHM channels (Table 1), it could have been difficult to demonstrate heteromultimer formation between CHM V369L and CHM channels at the whole-cell level, especially if the heteromultimers had small single-channel K^+ conductance and low P_o. However, when experiments were performed with a 1:10 concentration ratio between the CHM and the CHM V369L cRNAs, an experimental condition designed to increase the relative proportion of heteromultimers with respect to CHM homomultimers, no macroscopic current was detected. An identical 1:10 ratio of CHM L374V to CHM V369L cRNAs did not suppress the macroscopic currents, because of the formation of functional heteromultimers.

In addition, in order to directly test for the hypothesis that CHM V369L subunits did not form functional heteromultimers with CHM subunits, we performed single-channel experiments on oocytes coinjected with a 1:1 ratio of CHM V369L to CHM cRNA. In 14 patches (27 channels) analyzed, we observed a single population of channels that had a mean current amplitude of 1.58 ± 0.01 pA at 0 mV and 2.42 ± 0.03 pA at +40 mV (single-channel conductance for K^+ = 21.0 ± 0.7 pS). This channel population was indistinguishable from the CHM homomultimers, which had a mean current amplitude of 1.61 ± 0.01 pA at 0 mV and 2.42 ± 0.03 pA at +40 mV (single-channel conductance for K^+ = 21.9 ± 0.9 pS). The single class of channels observed in CHM V369L and CHM coinjected oocytes had gating properties identical to those of CHM homomultimers, characterized by long open times and large P_o (Table 1).

Even though we cannot exclude the possibility that CHM V369L/CHM heteromultimers were functionally identical to CHM homomers, these results strongly suggest that the formation of CHM V369L/CHM heteromultimers was either not occurring or, if occurring, was leading to nonfunctional channels.

Determination of the subunit stoichiometry of the heteromultimer formed upon coinjection of CHM V369L and CHM L374V cRNAs

As already mentioned, whole-cell measurements of the g_{Rb^+}/g_{K^+} ratio in oocytes coinjected with a 1:1 cRNA ratio for CHM V369L and CHM L374V or with CHM L374V cRNA alone are in close agreement with the values obtained from single-channel measurements of the g_{Rb^+}/g_{K^+} of the heteromultimer formed by CHM V369L and CHM L374V and for the CHM L374V homomer, respectively. This allowed us to

determine the subunit stoichiometry of the heteromultimer formed by CHM L374V and CHM V369L, from the dependence of the whole-cell g_{Rb^+}/g_{K^+} upon the ratio of the two cRNAs.

The results from these experiments (Fig. 7 *A*) show that even when a 100:1 ratio of CHM L374V to CHM V369L cRNAs was used, the normalized g_{Rb^+}/g_{K^+} ratio was lower than 0.3, indicating that most of the macroscopic current was still carried by the heteromultimeric CHM V369L/CHM L374V channels. Complete recovery of the CHM L374V homomer phenotype was only achieved in oocytes, which had been coinjected with a 100,000:1 ratio of CHM L374V to CHM V369L cRNAs.

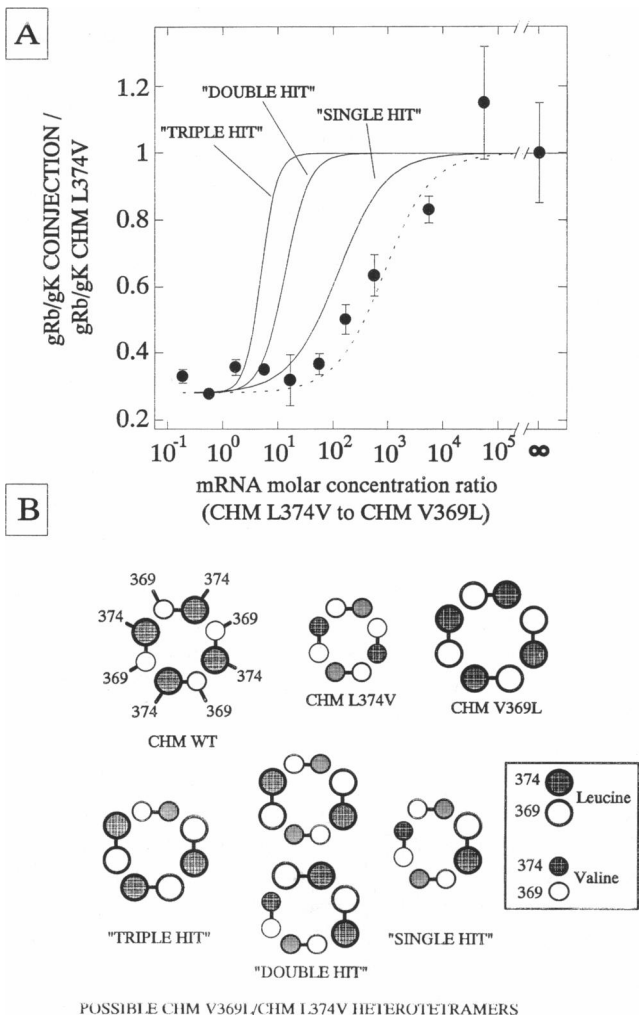

FIGURE 7 Determination of the subunit stoichiometry of the heteromultimer formed upon coinjection of CHM V369L and CHM L374V cRNAs. (*A*) *Xenopus* oocytes were injected with the indicated molar ratios of CHM L374V to CHM V369L cRNAs and the g_{Rb^+}/g_{K^+} ratio was estimated from normalized instantaneous I/V values recorded with high K^+-MES or high Rb^+-MES in the bath (see legends for Figs. 1 and 6). The solid lines are the theoretical predictions from the binomial statistics for the single, double, and triple hit heteromultimeric channels. The dotted line is the best fit to the experimental data obtained from Eq. A5 of the Appendix. As stated in the Appendix, the ordinate is the nondimensional Rb^+/K^+ conductance ratio (Γ_R) for each cRNA ratio (R), normalized to that of the CHM L374V homomer ($R = \infty$). (*B*) schematic diagram of the possible CHM V369L/CHM L374V heterotetramers formed upon coinjection of the cRNAs encoding for the two subunit species. Position 374 is indicated by filled symbols, while empty symbols indicate position 369. Large circles denote the presence of a leucine, while smaller circles indicate the presence of a valine.

At ratios between 1:10 and 10:1 of CHM L374V to CHM V369L, the characteristic single-channel currents of the heteromeric channel were unchanged. At higher ratios the number of heteromeric CHM V369L/CHM L374V channels relative to the number of homomeric CHM L374V channels became too low to make the search for heteromeric channels practical. Each heteromeric channel contributed 30 times the current of the homomeric channel so that the macroscopic currents were dominated by contributions of heteromeric channels despite the relative decrease in the ratio of heteromers to homomers.

As discussed in the Appendix, the results of the CHM V369L and CHM L374V coinjection ratio experiments, particularly the slope of the normalized g_{Rb^+}/g_{K^+} to cRNA ratio relationship, were consistent with the functional heteromultimer having a stoichiometry of three CHM L374V subunits and one CHM V369L subunit. However, the experimental midpoint of the normalized g_{Rb^+}/g_{K^+} to cRNA ratio relationship was right-shifted by a factor of about 6 when compared to the value expected if the assembly of the two types of subunits would occur in a totally random and independent fashion. This result can be interpreted as a consequence of either differential subunit production by the two cRNA species or of preferential subunit assembly occurring as a consequence of the differences in the pore regions of the two subunit types.

DISCUSSION

The results of the present study show that CHM V369L subunits, which are unable to form functional homomeric channels, can be assembled into functional heteromeric channels upon coexpression with CHM L374V subunits. We have obtained direct evidence at the single-channel level for this heteromultimeric assembly. A single class of functional heteromultimeric channels was observed, having a single-channel conductance for K^+, as well as gating and pharmacological properties clearly distinct from those of the CHM L374V homomer (Table 1). In fact, the K^+ conductance of the CHM V369L/CHM L374V heteromultimer was about 3 times larger than that of the CHM L374V homomer, while the Rb^+ conductance of the two channels was similar. With K^+ as the permeant ion, the mean open time of the CHM V369L/CHM L374V heteromeric channel was approximately 3 times longer than that of the CHM L374V homomer. This gating difference, together with a marked decrease in the mean closed times, led to a 10-fold increase in the P_o of the heteromultimer versus the CHM L374V homomer. In addition, the heteromultimeric channel displayed lower affinity for internal blockade by TEA when compared to CHM L374V homomers, while external TEA blockade

was unmodified. This result suggests that the architecture of the internal portion of the pore is affected, while externally accessible regions of the channel remain unmodified.

Several mechanisms could account for the inability of CHM V369L cRNA to express functional homomeric channels: 1) inability of the cRNA to be properly processed by the translation machinery; 2) inefficient assembly of the subunits into potentially functional channels; and 3) absence of permeation in correctly assembled channels. This last mechanism has been postulated to be responsible for the absence of ionic currents in a channel (ShakerB W434F) that had intact gating currents and opening and closing behavior (Perozo et al., 1993). However, we did not observe gating currents in oocytes injected with CHM V369L cRNA (M. Taglialatela, unpublished observations). This suggests that, if the homomeric CHM V369L channel is normally assembled, the mutation interferes with steps occurring before voltage-dependent gating. Also the first possibility, that the CHM V369L cRNAs are unable to be translated, seems unlikely since CHM L374V subunits can rescue CHM V369L subunits into functional heteromultimeric channels.

In the heteromeric channel, we have compensated for the changes induced by the CHM V369L mutation by a complementary CHM L374V mutation on a different subunit. This result indicates that the residues at positions 369 and 374 may interact not only within the same subunit (Kirsch et al., 1992b,c), but also between different subunits. The limited tolerance for interaction is supported by the present observation that a single class of functional heteromeric channels was detected despite the fact that three additional subunit combinations (Fig. 7 *B*) were possible for a heterotetrameric channel.

Interactions between subunit domains may affect assembly. The present results suggest that these interactions may not only involve the NH_2 terminus (Li et al., 1992) and leucine zippers (McCormack et al., 1991), but may involve the pore region as well. The fact that the experimental cRNA midpoint value for the g_{Rb^+}/g_{K^+} ratio determined from coinjection ratio experiments was right-shifted by a factor of 6 compared to the expectations of a binomial model of assembly may support this possibility. Recent experiments (Shen et al., 1993) have also demonstrated that K^+ channel subunits missing the NH_2 terminus recognition domain (Li et al., 1992) are still able to coassemble with subunits containing this domain, suggesting that other protein regions might be also important for subunit recognition.

The observation that single-channel currents of the heteromeric channel retained their characteristics over a 100-fold change in the cRNA ratios of injected CHM L374V seems to rule out an allosteric effect of the rescuing subunit. For allosteric regulation a graded change in single-channel currents should have occurred. Furthermore, the rescue of CHM V369L subunits into functional heteromultimers appeared to be highly specific since it was only observed upon coinjection with CHM L374V cRNA, not with CHM cRNA. This result seems inconsistent with an allosteric mechanism for the CHM V369L/CHM L374V heteromultimer. As discussed in the Appendix, for a tetrameric channel the results from the cRNA concentration ratio experiments would be most consistent with a stoichiometry of the heteromultimeric channel of 3 CHM L374V and 1 CHM V369L subunits. As shown in Table 1, the heteromultimeric channel has conduction, gating, and pharmacological properties, which are intermediate between the CHM L374V and the CHM homomers. Taken together, these results are consistent with the heteromeric channel having 2 Ls and 6 Vs, a configuration that is intermediate between the two functional homomeric channels CHM L374V (8 Vs) and CHM (4 Ls and 4 Vs). This configuration could have never been achieved using coinjection of CHM and CHM V369L cRNAs and may explain the absence of heteromultimers having functional properties distinct from those of CHM homomers.

There also appears to be specific positional sensitivity for the aliphatic residues V, I, and L that we have studied. The observation that the double CHM mutant, V369L + L374V, did not express functional channels indicates that position 369 in CHM is less tolerant of Ls than position 374. This would explain why the coinjection of the double mutant CHM V369L + L374V with CHM V369L was doomed.

With respect to the nature of the aliphatic residue at position 369 and 374 in the P-region of CHM, we may summarize the present results and our earlier results. CHM position 374 can accommodate 4 Ls (Hartmann et al., 1991), 4 Vs (Kirsch et al., 1992), and 4 Is (Taglialatela et al., 1993). CHM position 369 can accommodate 4 Vs (Hartmann et al., 1991), 4 Is (De Biasi et al., 1993), but according to the present results 1 or at most 2 Ls. The explanation may be that while L on the one hand and I or V on the other only have small differences in hydrophobicity and volume, they differ substantially in freedom of motion around their β-carbons. For L versus V or I, this is due to the ~0.5 Å difference in bond length between C-C and C-H (Pauling, 1967). Thus, very small changes in geometry at CHM P-region 369 have profound effects on channel function.

APPENDIX

A probabilistic model of heterotetrameric assembly of coexpressed ion channel subunits

(by J. P. Payne and M. Taglialatela)

The purpose of this appendix is to present a probabilistic model for the relative proportion of each multimeric species with respect to the relative amount of cRNA encoding for each subunit type. From this model, the stoichiometry of the functional heteromeric channel is derived from the dependence of the ratio of Rb^+ and K^+ conductances upon the ratio of the cRNA molar concentration of CHM L374V and CHM V369L. We will show that the functional heteromeric channel consists of 1 CHM V369L subunit and 3 CHM L374V subunits, but that assembly occurs nonrandomly.

i. Relative fraction of species in a heteromeric population—a binomial distribution model

The stoichiometry of a m-multimer resulting from the coexpression of two distinct types of monomeric subunits will obey a binomial distribution if (Walpole, 1982): 1) all multimers contain exactly m subunits and 2) subunits assemble in random order. The relative fraction of the channels that have j monomers of one subunit type and $m - j$ monomers of the other type to the total number of channels expressed on the cell surface, denoted by ν_j, can be expressed as

$$\nu_j = \binom{m}{j}\left(\frac{N_1}{N}\right)^j\left(\frac{N_2}{N}\right)^{m-j} \tag{A1}$$

where N is the total number of subunits in the pool available for assembly of which there are N_1 CHM L374V subunits and N_2 CHM V369L subunits and where j ranges from 0 to m. The term in parentheses of Eq. A1 represents the combinatorial coefficient. Assuming that a fully assembled channel is a tetramer, there are potentially five distinct channel types, denoted by: $j = 4$ for the CHM L374V homotetramer, 3 for the "single hit" heteromer, 2 for the "double hit" heteromer, 1 for the "triple hit" heteromer, and 0 for the CHM V369L homotetramer.

ii. The relationship between subunit number and cRNA concentration

An explicit relationship between subunit number and cRNA concentration can be developed as follows. Let C_n be the mass concentration, MW_n be the molecular weight, and V_n be the volume of cRNA suspension for the type n subunit injected into the host cell, where n is either 1 or 2 as in the previous section. The total number of copies of the type n cRNA injected is: $N_A C_n V_n / MW_n$, where N_A is Avogadro's number. If at steady-state there are n_n subunits of the type n made per initial copy of cRNA, then the total number of subunits of type n available for assembly is directly proportional to the cRNA molar concentration: $(n_n N_A V_n / MW_n)\ C_n$. If there is no selective degradation or translation of one type of cRNA over another nor differences in posttranslational modification, membrane targeting, or degradation of different protein subunits or assembled channels, then $n_1 = n_2$. Thus, the ratio of the number of protein subunits, N_1/N_2, is equal to the ratio of the molar concentration of the two types of cRNA, denoted by R. The relative fraction for the jth species, ν_j, becomes

$$\nu_j = \binom{m}{j}\frac{(R)^j}{(1+R)^m} \tag{A2}$$

For the coexpression of CHM L374V and CHM V369L ΔC318, the ratio of the cRNA molecular weights is 0.568, while for the full length the ratio is 1.

iii. The predicted Rb^+/K^+ conductance ratio for the binomial model heterotetramer

The experimental finding that only one new channel phenotype was observed upon coexpression of CHM L374V and CHM V369L cRNAs suggests that only one of the possible heteromeric channels was actually functional. Alternatively, channels with different stoichiometries have the same phenotype. We consider the former case explicitly and show that the latter case fails to improve the fit to the data.

The ratio of conductances for Rb^+ and K^+ for a mixed population of tetrameric K^+ channels of which only one heteromeric channel is functional in addition to the CHM L374V homomer is given by $\Gamma(R)$, where

$$\Gamma(R) = \frac{R^{m-j} + \binom{m}{j}\lambda\rho}{R^{m-j} + \binom{m}{j}\kappa\rho} \tag{A3}$$

where the dimensionless parameters given by

$$\rho = p_{o,j}/p_{o,4}$$

$$\kappa = \gamma_{K,j}/\gamma_{K,4}$$

$$\lambda = \gamma_{Rb,j}/\gamma_{Rb,4}$$

represent the ratio of the probability of opening at +40 mV (ρ), the ratios of the limiting K^+ (κ), and the Rb^+ (λ) conductances of the jth species relative to the CHM L374V ($j = 4$). Values for these parameters were directly obtained from single-channel measurements (Table 1).

There are two parameters that are useful in describing the behavior of $\Gamma(R)$ as a function of R in Eq. A3. One parameter is the cRNA ratio when both the jth heteromeric and the CHM L374V homomeric channels contribute equally to the observed conductance ratio, the cRNA midpoint, $R_{1/2}$, given by

$$R_{1/2} = \left[\binom{m}{j}\kappa\rho\right]^{1/(m-j)} \tag{A4}$$

For a given value of m, $R_{1/2}$ can discriminate which heteromultimer is the functional species. The converse establishes the total number of subunits incorporated into each m multimer. The other parameter is the slope of $\Gamma(R)$ at the cRNA midpoint. In a semilogarithmic plot of $\Gamma(R)$, the slope is directly related to the stoichiometry of the functional heteromer, given by: $(\ln 10)(m - j)(1 - \lambda/\kappa)/4$. For oligomeric ($m \leq 10$) channels, the midpoint slope can distinguish between single hit, double hit, etc. heteromers and thus identify the functional species.

For the single hit binomial model, the midpoint cRNA ratio is 107.5 (see Fig. 7 *B*). For the double hit binomial model, the midpoint cRNA ratio is shifted to the left about 9-fold, equal to 12.7, and in a semilog plot, the midpoint slope is twice that of the single hit model. For the triple hit, the curve is shifted the furthest to the left, with the midpoint

cRNA ratio equal to 4.75 and with a slope at the midpoint that is 3 times the single hit.

Comparing these results to the experimental data shows that the single hit model provides the closest fit, particularly with regard to the slope of the curve at the midpoint, although it underestimates $R_{1/2}$ by a factor of 6.

Although not shown, including the double hit and/or the triple hit in addition to the single hit heterotetramer does not significantly shift the cRNA midpoint. Thus, there is no compelling reason to believe that heteromers with different subunit stoichiometry have nearly identical phenotypes.

The inadequacy of the binomial model to predict the cRNA ratio midpoint value may be accounted for by: 1) differences in subunit production such that $n_2 > n_1$, 2) subunit aggregation is not random, or 3) the channel is not a tetramer. In the first case, the cRNA coding for CHM V369L would have to produce 6 times the number of subunits compared to CHM L374V in order to fit the experimental value of the cRNA midpoint. However, it is not clear how two conservative amino acid substitutions would dramatically alter the stability or translation efficiency of the coding mRNA or change posttranslational handling or degradation of the protein subunits. Furthermore, the fact that the same molar amount of cRNA encoding for both the full-length and the ΔC 318 version of the CHM L374V mutation generated the same amount of macroscopic current (see Results) seems to rule out any role for the COOH terminus in controlling translation efficiency or subunit assembly.

The possibility that the channel is not a tetramer does not seem to be supported by recent experimental data previously referred to (Li et al., 1992; Shen et al., 1993). The remaining possibility that different subunits preferentially associate during assembly is considered in detail.

iv. The effect of preferential subunit assembly

To provide the greatest generality of the model, preferential subunit association is modeled as a limited polymerization reaction governed by a set of kinetic rate constants (Hill, 1987) (Fig. 8). The assembled channel is assumed to be a tetramer. Recognizing that only fully assembled channels are observable, all the equilibrium constants are assumed to be identical, except for reactions which form tetrameric species. Because only the single hit heterotetramer and the CHM L374V homomer are considered to be functional channels, the single hit nondimensional conductance ratio is now given by

$$\Gamma(R) = \frac{1 + (N_8^e(R)/N_5^e(R))\lambda\rho}{1 + (N_8^e(R)/N_5^e(R))\kappa\rho} \qquad (A5)$$

where $N_5^e(R)$ and $N_8^e(R)$ are the numbers of CHM L374V homotetramers and single hit heterotetramers at equilibrium and R again represents the cRNA molar concentration ratio.

The simplest explanation that accounts for the rightward shift of the experimental cRNA midpoint requires that only the reaction generating the single hit heterotetramer be positively cooperative. Preferential subunit binding can then be expressed in terms of a scaling factor σ, equal to K_{48}/K_{45}, which represents the thermodynamic cooperativity of binding (Goldstein and Stryer, 1986). Fitting the cRNA midpoint gives a value of 40.8855 for σ, which corresponds to a difference of −2.175 kcal/mol between the formation of a single hit heterotetramer and the CHM L374V homotetramer. Interestingly, this difference in binding energy is rather small, being on the order of a single methyl group binding to a protein, −2.0 to −3.9 kcal/mol (Creighton, 1993). Using this value for σ, solutions for other values of R will generate a curve that closely fits the experimental data (Fig. 7 *B*).

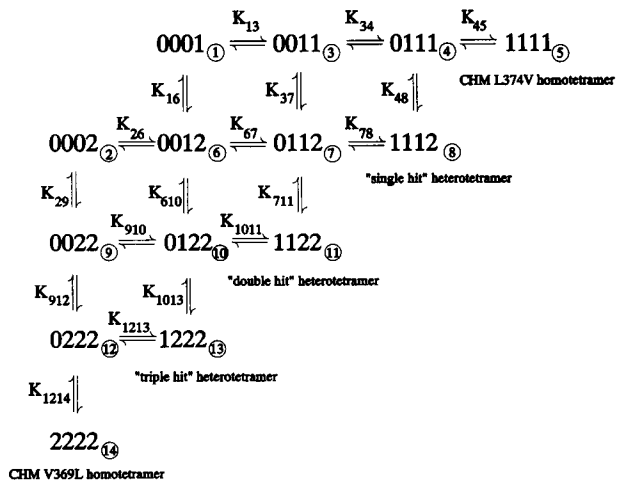

FIGURE 8 A kinetic diagram for tetrameric channel assembly. Legend for stoichiometry of the 14 species of homo- and heterodimers, trimers, and tetramers: 0 = unoccupied position, 1 = CHM L374V subunit, 2 = CHM V369L subunit. The subscript in the circle is the cataloguing index for that species. The binding of a type i monomer to the jth species is described by: $K_{jk} = N^e_k/N^e_i N^e_j$, where N^e represents the number of that species present at equilibrium and index k denotes the product. Note that K_{jk} is not a true binding constant as it relates the absolute number of molecules, not their concentration; however, ratios of these constants are physically significant and can be related to differences of binding free energy (see Appendix for details).

v. Conclusion

In this Appendix, we have attempted to establish the stoichiometry of the CHM V369L/CHM L374V heteromultimer by measuring the Rb^+/K^+ conductance ratio in oocytes injected with various cRNA ratios.

A probabilistic model for heteromultimeric channel assembly can accurately fit the experimental data for the cRNA midpoint slope, suggesting that the functional heterotetramer is composed of 3 CHM L374V and 1 CHM V369L subunits. However, the experimental cRNA midpoint value for this single hit heteromultimer was right-shifted by a factor of 6. This shift can be interpreted in terms of nonindependent subunit assembly, presumably occurring as a consequence of differences in pore structure.

The authors wish to thank Gaby Schuster and Wei-Qiang Dong for oocyte injections and handling and Mary Champagne and Merry Lindsey for molecular biology technical support.

This work was supported in part by National Institutes of Health grants NS23877 and HL36930 and by Texas Higher Education Board Advanced Technological Program (ATP) grant 004949-032 to A. M. Brown.

REFERENCES

Armstrong, C. M. 1971. Interaction of tetraethylammonium ion derivatives with the potassium channel of the squid axon. *J. Gen. Physiol.* 58: 413–437.

Christie, M. J., R. A. North, P. B. Osborne, J. Douglass, and J. P. Adelman. 1990. Heteropolymeric potassium channels expressed in *Xenopus* oocytes from cloned subunits. *Neuron.* 2:405–411.

Creighton, T. E. 1993. Proteins, Structures, and Molecular Properties. 2nd ed. W. H. Freeman and Co., New York.

DeBiasi, M., H. A. Hartmann, J. A. Drewe, M. Taglialatela, A. M. Brown, and G. E. Kirsch. 1993. Inactivation determined by a single site in K^+ pores. *Pflügers Arch. Eur. J. Physiol.* 422:354–363.

Frech, G. C., A. M. J. VanDongen, G. Schuster, A. M. Brown, and R. H. Joho. 1989. A novel potassium channel with delayed rectifier properties isolated from rat brain by expression cloning. *Nature (Lond.).* 340: 642–645.

Goldstein, R. F., and L. Stryer. 1986. Cooperative polymerization reactions. *Biophys. J.* 50:583–599.

Hartmann, H. A, G. E. Kirsch, J. A. Drewe, M. Taglialatela, R. H. Joho, and A. M. Brown. 1991. Exchange of conduction pathways between two related K^+ channels. *Science (Wash. DC).* 251:942–944.

Hill, T. L. 1987. Linear Aggregation Theory in Cell Biology. Springer-Verlag, New York.

Isakoff, E. Y., Y. N. Jan, and L. Y. Jan. 1990. Evidence for the formation of heteromeric potassium channels in Xenopus oocytes. *Nature (Lond.).* 345:530–534.

Joho, R. H., J. R. Moorman, A. M. J. VanDongen, G. E. Kirsch, H. Silberberg, G. Schuster, and A. M. Brown. 1990. Toxin and kinetic profile of rat brain type III sodium channels expressed in *Xenopus* oocytes. *Mol. Brain Res.* 7:105–113.

Kavanaugh, M. P., R. S. Hurst, J. Yakel, M. D. Varnum, J. P. Adelman, and R. A. North. 1992. Multiple subunits of a voltage-dependent potassium channel contribute to the binding site for tetraethylammonium. *Neuron.* 8:493–497.

Kirsch, G. E., J. A. Drewe, H. A. Hartmann, M. Taglialatela, M. De Biasi, A. M. Brown, and R. H. Joho. 1992*a*. Differences between the deep pores of K^+ channels determined by an interacting pair of non-polar amino acids. *Neuron.* 8:499–505.

Kirsch, G. E., J. A. Drewe, M. Taglialatela, M. DeBiasi, H. A. Hartmann, and A. M. Brown. 1992*b*. A single non-polar residue in the deep pore of related K^+ channels acts as a K^+:Rb^+ conductance switch. *Biophys. J.* 62:136–144.

Kirsch, G. E., J. A. Drewe, M. DeBiasi, M. Taglialatela, H. A. Hartmann, and A. M. Brown. 1992*c*. Functional interaction between subunits of a chimeric K^+ channel. *Soc. Neurosci. Abstr.* 18:1094.

Kirsch, G. E., M. Taglialatela, and A. M. Brown. 1991. Internal and external TEA block in single cloned K^+ channels. *Am. J. Physiol.* 30:C583–C590.

Li, M., Y. N. Jan, and L. Y. Jan. 1992. Specification of subunit assembly by the hydrophilic amino-terminal domain of the Shaker K^+ channel. *Science (Wash. DC).* 257:1225–1230.

MacKinnon, R. 1991. Determination of the subunit stoichiometry of a voltage-activated potassium channel. *Nature (Lond.).* 350:232–235.

Maniatis, T., E. F. Fritsch, and J. Sambrook. 1989. Molecular Cloning. A Laboratory Manual. 2nd Ed. Cold Spring Harbor Laboratory, Cold Spring Harbor, New York. Sections 1–18.

McCormack, K., M. A. Tanouye, L. E. Iverson, L. E., J. Lin, M. Ramaswami, T. McCormack, J. T. Campanelli, M. K. Mathew, and B. Rudy. 1991. A role for hydrophobic residues in the voltage-dependent gating of Shaker K^+ channels. *Proc. Natl. Acad. Sci. USA.* 88:2931–2935.

Noda, M., S. Shimuzi, T. Tanabe, et al. 1984. Primary structure of Electrophorus electricus sodium channel deduced from cDNA sequence. *Nature (Lond.).* 312:121–127.

Pauling, L. 1967. The Nature of the Chemical Bond. Table 7.2, p224. Cornell University Press.

Perozo, E., R. MacKinnon, F. Bezanilla, and E. Stefani. 1993. Gating currents from a non-conducting mutant reveal open-closed conformations in *Shaker* K^+ channel. *Neuron.* 11:353–358.

Po, S., S. Roberds, D. J. Snyders, M. M. Tamkun, and P. B. Bennet. 1993. Heteromultimeric assembly of human potassium channels. Molecular basis of a transient outward current? *Circ. Res.* 72:1326–1336.

Richards, F. M. 1977. Areas, volume, packing, and protein structure. *Annu. Rev. Biophys. Bioeng.* 6:151–176.

Ruppersberg, J. P., K. H. Schroter, B. Sakmann, M. Stocker, S. Sewing, and O. Pongs. 1990. Heteromultimeric channels formed by rat brain potassium channel proteins. *Nature (Lond.).* 345:535–537.

Sala, S. and D. R. Matteson. 1991. Voltage-dependent slowing of K^+ channel closing kinetics by Rb^+. *J. Gen. Physiol.* 98:535–554.

Salkoff, L., K. Baker, A. Butler, M. Covarrubias, M. Pak, and A. Wei. 1992. An essential "set" of K^+ channels conserved in flies, mice and humans. *Trends Neurosci.* 15:161–166.

Shen, N.V., X. Chen, M. M. Boyer, and P. J. Pfaffinger. 1993. Deletion analysis of K^+ channel assembly. *Neuron.* 11:67–76.

Schwartz, T. L., B. Tempel, D. M. Papazian, Y. N. Jan, and L. Y. Jan. 1988. Multiple potassium channel components are produced by alternative splicing at the Shaker locus of *Drosophila. Nature (Lond.).* 331:137–142.

Shapiro, M. S. and T. E. DeCoursey. 1991. Permeant ion effects on the gating kinetics of the type L potassium channel in mouse lymphocytes. *J. Gen. Physiol.* 97:1251–1278.

Shen, N. V., X. Chen, M. M. Boyer, and P. J. Pfaffinger. 1993. Deletion analysis of K^+ channel assembly. *Neuron.* 11:67–76.

Tanabe, T., H. Takeshima, A. Mikami, V. Flockerzi, H. Takahashi, M. Koijma, H. Matsuo, T. Hirose, and S. Numa. 1987. Primary structure of the receptor for calcium channel blockers from skeletal muscle. *Nature (Lond.).* 328:313–318.

Taglialatela, M., A. M. J. VanDongen, J. A. Drewe, R. H. Joho, A. M. Brown, and G. E. Kirsch. 1991. Patterns of internal and external tetraethylammonium block in four homologous K^+ channels. *Mol. Pharmacol.* 40:299–307.

Taglialatela, M., J.A. Drewe, G.E. Kirsch, M. DeBiasi, H.A. Hartmann, and A.M. Brown. 1993. Regulation of K^+/Rb^+ selectivity and internal TEA blockade by mutations at a single site in K^+ pores. *Pflügers Arch. Eur. J. Physiol.* 423:104–112.

VanDongen, A. M. J. 1992. Transit: a new algorithm for analyzing single ion channel data containing multiple conductance levels. *Biophys. J.* 61: 256*a*. (Abstr.)

VanDongen, A. M. J., G. C. Frech, J. A. Drewe, R. H. Joho, and A. M. Brown. 1990. Alteration and restoration of K^+ channel function by deletions at the N- and C-termini. *Neuron.* 4:433–443.

Walpole, R. E. 1982. Introduction to Statistics. 3rd ed. Macmillan, New York. 57–63.

Yellen, G., M. Jurman, T. Abramson, and R. MacKinnon. 1991. Mutations affecting internal TEA blockade identify the probable pore-forming region of a K^+ channel. *Science (Wash. DC).* 251:939–942.

Yokoyama, S., K. Imoto, T. Kawamura, H. Higashida, N. Iwabe, T. Miyata, and S. Numa. 1989. Potassium channels from NG108–15 neuroblastoma-glioma hybrid cells. *FEBS Lett.* 259:37–42.

Yool, A. J., and T. L. Schwarz. 1991. Alteration of ionic selectivity of a K^+ channel by mutation of the H5 region. *Nature (Lond.).* 349:700–704.